Tracking saddle-to-scission dynamics using N/Z in projectile breakup reactions

S. Hudan, A. B. McIntosh, R. T. de Souza, S. Bianchin, J. Black, A. Chbihi, M. Famiano, M. O. Frégeau, J. Gauthier, D. Mercier, J. Moisan, C. J. Metelko, R. Roy, C. Schwarz, W. Trautmann, and R. Yanez

Phys. Rev. C **86**, 021603 — Published 13 August 2012

DOI: 10.1103/PhysRevC.86.021603

Tracking saddle-to-scission dynamics using N/Z in projectile breakup reactions

S. Hudan,[1] A. B. McIntosh,[1] R. T. de Souza,[1,*] S. Bianchin,[2] J. Black,[1] A. Chbihi,[3] M. Famiano,[4] M. O. Frégeau,[5] J. Gauthier,[5] D. Mercier,[1,†] J. Moisan,[5] C. J. Metelko,[1,‡] R. Roy,[5] C. Schwarz,[2] W. Trautmann,[2] and R. Yanez[1,§]

[1] *Department of Chemistry and Center for Exploration of Energy and Matter*
2401 Milo B. Sampson Lane, Bloomington IN 47405, USA
[2]*GSI Helmholtzzentrum GmbH, Planckstr. 1, D-64291 Darmstadt, Germany*
[3]*GANIL, Caen, France*
[4]*Western Michigan University, Kalamazoo, MI, USA*
[5]*Université Laval, Québec, Canada*

(Dated: July 26, 2012)

Fragments produced in binary splits of an excited projectile-like fragment (PLF*) formed in the reactions ^{124}Xe + ^{112,124}Sn at an incident energy of 50 MeV/A are examined. The dependence of the isotopic composition of light fragments ($4 \leq Z_L \leq 8$) on rotation angle allows one to explore changes in N/Z on the timescale of the rotational period of the PLF*. Changes in the N/Z of the fragments persist for times as long as 2-3 zs (600-900 fm/c). The two component nature of the time dependence of $\langle N \rangle /Z$ for Z_L=4 and the Z dependence are related to differences in the initial configurations and subsequent decay of the PLF*.

PACS numbers: 25.70.Mn, 25.70.Lm, 21.65.Ef

The density dependence of the nuclear symmetry energy impacts a broad range of phenomena from the composition of a neutron star crust to the formation of heavy elements in a supernova explosion [1–3]. One probe of the density dependence of the nuclear symmetry energy is the preferential transport of neutrons from regions of high density to regions of low density [4, 5]. On general grounds probing this density dependence is favored by examining a system that is sufficiently long lived to sense the underlying density-dependent potential. The dinuclear systems formed in strongly damped collisions of two heavy-ions, either N/Z symmetric [6] or N/Z asymmetric [7], present such an opportunity. While neutron and proton transport in strongly damped collisions has been the focus of several investigations in the 1980's [8, 9], the density dependence of the underlying potential was not considered. To establish the characteristic timescale of N/Z equilibration, we therefore focus in this initial work on examining systems which are sufficiently long lived.

Peripheral collision of the projectile and target nuclei at intermediate energies results in the formation of an excited, transiently deformed projectile-like fragment, denoted the PLF*, which can subsequently decay into two or more large fragments [10–14]. This decay mode is reminiscent of low-energy fission modified by the collision dynamics. Governed by its spin and lifetime, the decaying PLF* exhibits a characteristic angular distribution. Aligned breakup occurs with characteristic correlations between the size and velocity of the fragments [12], on the timescale of ≈300 fm/c [13, 15, 16]. It is reasonable to assume that since regions of low and high density exist during the collision phase, that these regions persist and continue to equilibrate during this secondary stage. In this work we examine for the simplest case of binary decay of the projectile-like fragment, whether N/Z equilibration occurs after the initial separation of the projectile-like and target-like fragments. Moreover, using the rotational period of the projectile-like fragment as a clock, we extract the timescale for N/Z equilibration.

The experiment was conducted at the GANIL facility in Caen, France, where beams of ^{124,136}Xe ions accelerated to E/A = 50 MeV impinged on ^{112,124}Sn targets 800 μg/cm^2 thick with an average beam intensity of $\approx 10^8$ p/s. The experimental details of the experiment have been previously published [16] and are summarized below for completeness. Charged products of the reaction were identified by the array FIRST [17],which subtended the angular range $3^\circ \leq \theta_{lab} \leq 14^\circ$. The forward telescope in FIRST spanned the angular range $3^\circ \leq \theta_{lab} \leq 7^\circ$ and provided identification by atomic number of all products up to Z=55 and isotopic information for Z ≤ 14. The larger angle telescope in FIRST provided Z identification for Z ≤ 24 and A identification for Z ≤ 8. The high segmentation of FIRST provided an angular resolution of $\pm 0.05^\circ (3^\circ \leq \theta_{lab} \leq 7^\circ)$ and $\pm 0.44^\circ (7^\circ \leq \theta_{lab} \leq 14^\circ)$ in polar angle and $\pm 11.25^\circ$ in azimuthal angle. The energy resolution obtained was approximately 1%.

To focus on binary decays, events were selected in which two fragments (Z ≥ 4) were detected within the laboratory angular range $3^\circ \leq \theta_{lab} \leq 14^\circ$. The two fragments were distinguished by their atomic number, with the larger (smaller) atomic fragment designated as Z_H (Z_L). In addition, in order to ensure that the PLF* under investigation comprised a large fraction of the initial projectile, events selected were required to have $Z_H > 20$. Selection of these events corresponds to approximately

*Electronic address: desouza@indiana.edu
†Present address: Riken, Japan
‡Present address: Particle Physics Dept., Rutherford Appelton Labs., Didcot, UK
§Present address: Department of Chemistry, Oregon State University, Corvallis, OR, 97331, USA

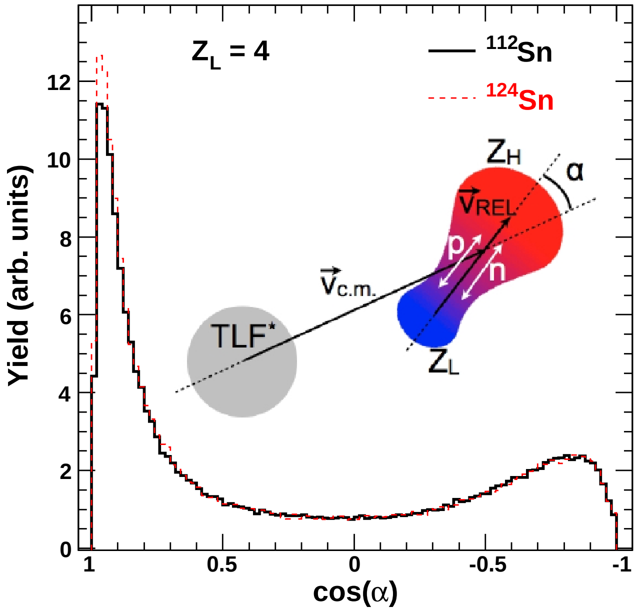

FIG. 1: (Color online) The angular distribution of binary splits (Z_L-Z_H) for Z_L=4, representative of other fragments, is shown. Data for the ^{124}Xe + ^{112}Sn and ^{124}Xe + ^{124}Sn systems are represented by the black, solid and red, dashed histograms respectively.

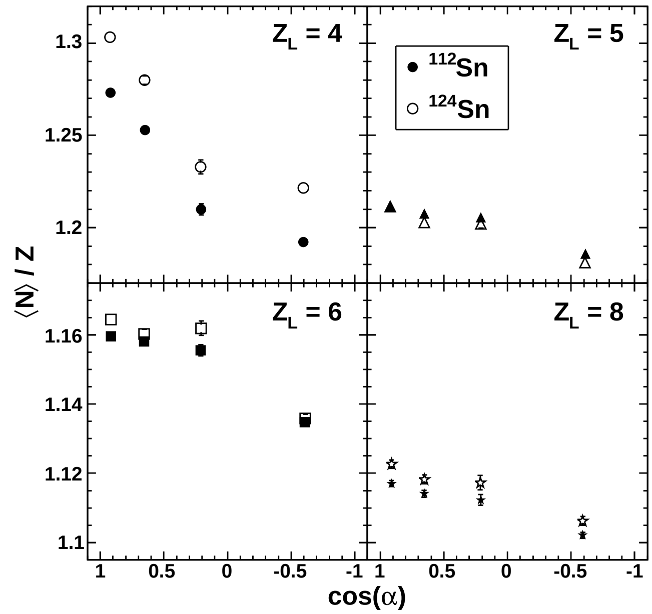

FIG. 2: Panel (a-d) Isotopic composition for different Z_L fragments in the ^{124}Xe + ^{112}Sn system (closed symbols) and ^{124}Xe + ^{124}Sn system (open symbols) as a function of their decay angle.

20% of the measured yield in which one fragment with Z>20 was detected. In contrast to previous work [16], as we are interested in using the rotation of the PLF* as a clock, we extend our analysis from the angular range 3° $\leq \theta_{lab} \leq$ 7° to a broader angular range of 3° $\leq \theta_{lab} \leq$ 14°.

A simple characteristic quantity for defining the binary decay is the angle between the direction of the two fragments center-of-mass velocity, $v_{c.m.}$ and their relative velocity, v_{REL} [11, 16]. We construct this angle α, as indicated within the inset of Fig. 1, with the relative velocity vector, v_{REL}, defined as v_{REL}=v_H-v_L. Consequently, aligned decays with Z_L emitted backward (forward) of Z_H correspond to cos(α) = 1 (-1). Momentum correlations observed between Z_H and Z_L reveal that these two fragments originate from a common parent [16]. This parent nuclear system comprised of Z_H and Z_L is designated as the PLF*. Previous studies have demonstrated that the PLF* is an elongated, rapidly rotating transient system which subsequently decays [11, 15, 18, 19].

A defining feature of the binary decay of the PLF* at intermediate energies is the enhancement in yield for backward emission from the PLF* relative to forward emission [10, 11, 20]. In Fig. 1 we present the angular distributions for Z_L= 4 within the angular range of this analysis. Data for the ^{124}Xe + ^{112}Sn system is represented by the black solid line histogram. The angular distribution presented is markedly asymmetric with a large enhancement in yield for backward emission (cos(α)=1). Moreover, this yield enhancement in the backward direction is also characterized by a narrow peak, indicating a strong alignment of v_{REL} relative to $v_{c.m.}$. While both the yield enhancement and the alignment decrease as Z_L increases, they persist up to Z_L = 18. Also shown in Fig. 1 is the angular distribution for the ^{124}Xe + ^{124}Sn system indicated by the dashed red histogram. The distribution for the ^{124}Sn target has been area normalized in the range -1 $\leq$ cos(α) $\leq$ 0 to the ^{112}Sn target data. With this normalization it is observed that the angular distributions for the two targets are virtually identical. In effect the two targets manifest the same yield enhancement as a function of angle. We therefore do not observe a dependence of the backward emission probability on the target composition. This result is in contrast to published results for dynamical emission in Sn+Ni reactions [21]. In the case of the Sn+Ni reactions however both the N/Z of the target and the projectile were simultaneously varied.

Depicted in Fig. 2 is the angular dependence of the isotopic composition of different elements. A clear trend is evident for all Z_L shown in Fig. 2. For all fragments emitted at backward angles, an enhancement in ⟨N⟩/Z is observed as compared to the forward direction (-1 $\leq$ cos(α) $\leq$ 0). This enhancement is most striking for Z_L = 4. For the case of Z_L = 4, at the most backward angles one observes that ⟨N⟩/Z is enhanced relative to the forward direction by 7%. As the rotation angle increases, this enhancement in ⟨N⟩/Z decreases monotonically. For Z_L > 4, while an enhancement is still observed, the magnitude of the enhancement is smaller than for Z_L = 4. The ⟨N⟩/Z values observed for forward emission are consistent with values previously observed in projectile fragmentation studies at 600 MeV/A [22]. Data for the ^{124}Xe

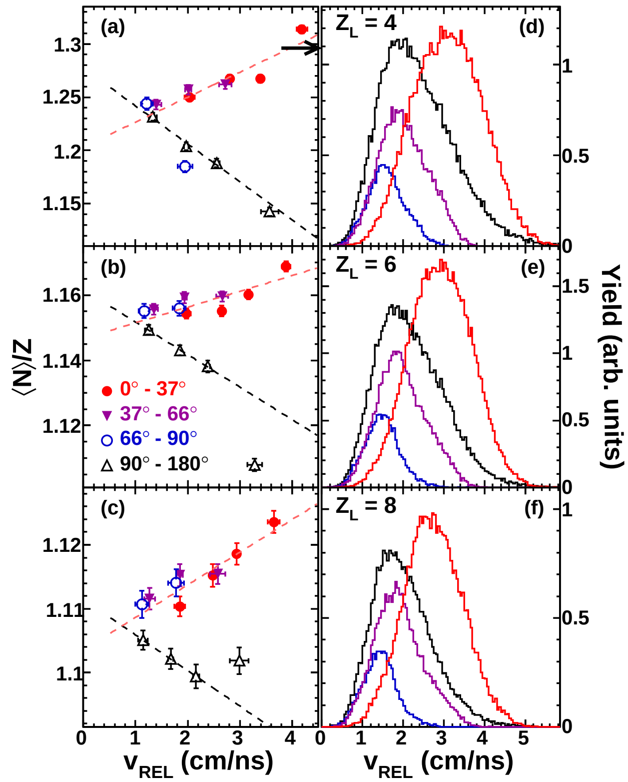

FIG. 3: (Color online) Left column: Dependence of ⟨N⟩/Z on v_{REL} for Z_L=4,6, and 8 in the four angular ranges. Lines serve to guide the eye. Right column: Distributions of v_{REL} for the indicated fragments in the angular ranges indicated.

+ ^{124}Sn system (open symbols) manifests a similar enhancement as did the ^{124}Xe + ^{112}Sn system (closed symbols). For the neutron-rich ^{124}Sn target, slightly larger values of ⟨N⟩/Z are observed for most fragments, particularly Z_L=4. Although changing the target from ^{112}Sn to ^{124}Sn corresponds to an increase of ≈20% in N/Z, only a relatively small enhancement is observed for the ⟨N⟩/Z of the fragments. The similarity of the two systems suggests that the neutron content of the target does not play a dominant role in either the yield (Fig. 1) or the composition, ⟨N⟩/Z, of the fragments emitted backward in the decay of the PLF*.

Before utilizing the rotation angle as a clock to extract the time dependence for ⟨N⟩/Z, it is necessary to consider other factors that might influence the evolution of N/Z. While short-lived dynamical decays preferentially populate backward angles, $\alpha<90°$, as compared to forward angles, $\alpha>90°$, decays that are long-lived compared to the rotational period of the PLF* are more isotropic in character. As dynamical decays are characterized by a larger relative velocity as compared to a Coulomb dominated picture [10, 11], we decided to investigate whether there is an association between ⟨N⟩/Z and v_{REL} for different angular cuts. The results are presented in the left-hand column of Fig. 3. For fragments with Z_L=4, 6, and 8 selected on four angular ranges in α, the dependence of ⟨N⟩/Z on v_{REL} is depicted. For forward emission, $90°\leq\alpha<180°$, denoted by the black symbols, ⟨N⟩/Z decreases as v_{REL} increases. This trend, observed for all $4\leq Z_L\leq 8$, is qualitatively consistent with a Coulomb effect in which neutron-deficient isotopes of a particular element acquire a larger velocity from an emitting source due to their lower mass [23]. In marked contrast to this trend is the overall trend observed for backward emission, $\alpha<90°$. In this case, the ⟨N⟩/Z decreases with decreasing v_{REL}. It is noteworthy that different angular cuts in this range follow a similar dependence. As the Coulomb effect observed for forward emission is also expected to be present for backward emission, though possibly with a reduced magnitude, the observed ⟨N⟩/Z at a given v_{REL} represents a lower limit for the ⟨N⟩/Z. The lone data point that violates this trend is for Z_L=4 and $66°\leq\alpha<90°$ with $v_{REL}\approx 2$ cm/ns. For reference the N/Z=1.3 of the projectile is shown as an arrow in the figure. To indicate the relative yield associated with each of the angular cuts, the distribution of v_{REL} for each angular cut is shown in the right-hand column of Fig. 3. A significant yield is observed for each of the cases, indicating the trends observed are not for rare events.

Within a simple picture the fission-like binary decay of the PLF* is governed by a rotational frequency and a lifetime. Thus, for a given rotational frequency a specific angle can be related to a specific time. The rotational frequency for the dinuclear PLF* complex was taken to be linear with Z for Z_L = 4-8 in the range of 0.7-0.6 x 10^{21}rad/s. This rotational frequency was taken from prior experimental analyses for similar systems and corresponds to a rotational angular momentum of the dinuclear PLF* complex of $\ell\approx 40\ \hbar$ [15]. The moment of inertia of the dinuclear complex is taken to be that of two touching ellipsoids with a value of 0.6 for the ratio of the minor to major axes [15].

In order to relate the observed dependence of ⟨N⟩/Z on v_{REL} to a dependence on time, we examined the relationship between v_{REL} and cos(α). For Z_L=4, the average v_{REL} decreases monotonically from 3.7 cm/ns for the most backward decays to ≈ 1.5 cm/ns for transverse decays. A similar dependence is observed for other Z_L. The dependence of $\langle v_{REL}\rangle$ on cos(α) was parametrized for each Z_L.

The resulting dependence of ⟨N⟩/Z on time is shown in Fig. 4. The timescale is expressed in zeptoseconds (1zs = 1x10^{-21}s) with the longest times extracted corresponding to a quarter rotation of the PLF*. The observation that N/Z equilibration between Z_H and Z_L persists up to 3 zs (900 fm/c) indicates the slow nature of this equilibration process. These observed timescales are longer than those previously published [16] due to the larger angular acceptance of the present analysis. For Z_L=4 a clear trend is observed with ⟨N⟩/Z decreasing from ≈1.31 at the shortest times to ≈1.24 at the longest times. Closer examination of the data for Z_L=4 reveals a hint of two timescales. The most aligned decays $0°\leq\alpha<37°$ exhibit a more rapid decrease with time than decays in the an-

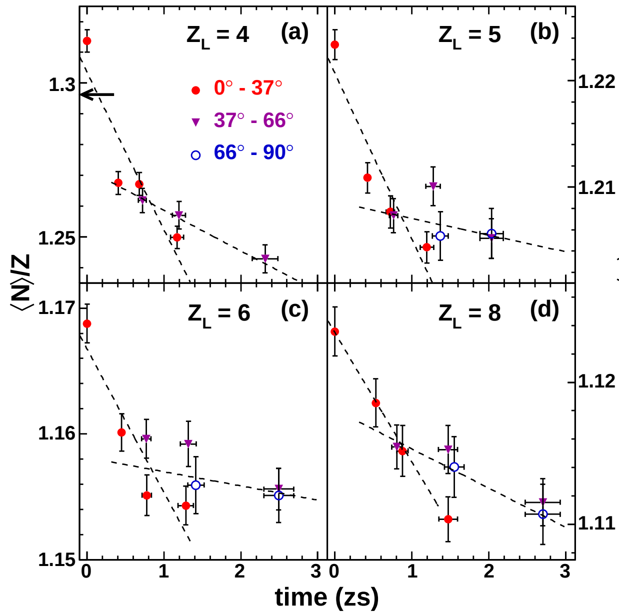

FIG. 4: (Color online) Dependence of the ⟨N⟩/Z on time for $4 \leq Z_L \leq 8$. See text for details.

gular range 37°≤α<66°. To make the observed trend more evident, we have performed a linear fit to the measured data in two time intervals, 0≤t≤1 zs and t≥0.5 zs. The resulting fits are shown as dashed lines in the figure. While a similar overall trend is observed for Z_L=8 fragments, the change in ⟨N⟩/Z for both short and long times is comparable. Although a similar overall behavior is observed for fragments with Z_L=5 and 6, in these cases the trend is somewhat less clear cut. In particular, the trend for these latter fragments depends more heavily on the large ⟨N⟩/Z at the shortest times. Considering the clear trends evident for Z_L=4 and 8 however, it is reasonable to presume an overall decrease in ⟨N⟩/Z as time increases for fragments with $4 \leq Z_L \leq 8$.

These results can be understood within the following physical scenario. Peripheral collision of the projectile and target nuclei results in a deformed, rotating projectile-like fragment which can subsequently undergo a fission-like decay. From this perspective, the two important configurations (and the corresponding moments in time) are the saddle point and the scission point on a potential energy surface. The abscissa in such a potential energy diagram is a reaction coordinate that can be related to an elongation parameter of the configuration. A long fission time scale has been inferred from the measured multiplicities of pre-scission neutrons in fusion-fission reactions [24]. Within the context of a statistical model [25, 26], these long fission time scales can be interpreted as due to strongly overdamped motion as the system evolves towards scission. While we do not know *a priori* the initial configuration of the PLF*, for a given rotation angle α, a distribution of initial configurations exists. Some configurations are stretched with less overlap of the emerging Z_L and Z_H fragments, i.e. closer to scission. Other initial configurations are more compact shapes with a larger overlap of the two emerging nuclei. The latter configurations are closer to the saddle point of the decaying system. It is reasonable to assume that the more stretched configurations proceed to scission more quickly, hence undergo only a small rotation of the PLF* system. In contrast, the more compact configurations, with a larger distance from the initial configuration to scission to traverse (in elongation parameter), survive for longer and consequently experience a larger degree of rotation. The two timescale nature for the Z_L=4 fragments suggests that for these fragments perhaps a bimodal set of initial configurations exists both those that are stretched, as well as those that are compact. In contrast, for Z_L=8 fragments the distribution of initial configurations is more homogeneous and favors more compact distributions. This physical picture is consistent with an earlier work [16] which deduced that heavier fragments such as Z_L=8 were associated with initial configurations closer to the saddle than to scission than in the case for light fragments (Z_L=4). These prior conclusions were based only upon the degree of alignment of the decaying system and a more limited angular range.

Two principal factors influence the evolution of ⟨N⟩/Z with time. The first factor is any initial N/Z asymmetry between the nascent Z_H and Z_L fragments, while the second factor is the existence of a low-density region in the middle of the dinuclear system combined with a density-dependent symmetry energy. It has previously been established that a net preferential flow of neutrons to low density occurs for a system initially symmetric in both A and N/Z [6]. Whether the observed decrease of ⟨N⟩/Z with time for a given Z_L is due to preferential neutron transport to the low-density region, exchange with the normal-density Z_H fragment, or neutron emission as the descent from initial configuration to scission occurs, is presently unclear. Isotopic identification of both the Z_H and Z_L fragments together with measurement of free neutrons could resolve this ambiguity.

We have established that fragments produced in the dynamical binary breakup of a PLF* exhibit a correlation of their ⟨N⟩/Z with rotation angle. Moreover, the isotopic composition of light fragments emitted backward and forward in the decay of the PLF* manifests a different v_{REL} dependence. The trend of decreasing ⟨N⟩/Z with increasing v_{REL} for forward emission can be qualitatively understood as a Coulomb effect. In contrast, backward decays manifest the opposite trend, namely a decreasing ⟨N⟩/Z with decreasing v_{REL}. Within the uncertainty of the measurement, the magnitude of this trend is the same for all angular cuts. The extracted time dependence of ⟨N⟩/Z reveals that the composition of Z_L continues to decrease for times as long as 2-3 zs (600-900 fm/c). The continuous evolution of ⟨N⟩/Z on such long timescale is only accessible because of the relatively long-lived dinuclear complex. Differences in the time dependence of ⟨N⟩/Z for Z_L=4 and Z_L=8 fragments may be related to differences in the initial dinuclear configurations and their lifetime. This result suggests that damped reactions at low energy radioactive beam facilities may present new opportunities in studying the density dependence of the nuclear symmetry energy.

Acknowledgments

We wish to acknowledge the support of the GANIL staff in providing the high quality beam that made this experiment possible. We are especially grateful to Y. Georget, B. Jacquot, and V. Morel. This work was supported by the U.S. Department of Energy under Grant No. DEFG02-88ER-40404 (IU) and by the National Science Foundation under Grant No. PHY-1064280 (WMU). Collaboration members from Université Laval recognize the support of the Natural Sciences and Engineering Research Council of Canada.

---

[1] J. Lattimer and M. Prakash, Astrophys. J. **550**, 426 (2001).
[2] A. Steiner et al., Phys. Rep. **411**, 325 (2005).
[3] H. T. Janka et al., Phys. Rep. **442**, 38 (2007).
[4] B. A. Li, Phys. Rev. C **69**, 034614 (2004).
[5] V. Baran et al., Phys. Rev. C **72**, 064620 (2005).
[6] D. Thériault et al., Phys. Rev. C **74**, 051602 (R) (2006).
[7] M. B. Tsang et al., Phys. Rev. Lett. **92**, 062701 (2004).
[8] R. T. deSouza et al., Phys. Rev. C **37**, 1783 (R) (1988).
[9] R. Planeta et al., Phys. Rev. C **41**, 942 (1990).
[10] F. Bocage et al., Nucl. Phys. A. **676**, 391 (2000).
[11] B. Davin et al., Phys. Rev. C. **65**, 064614 (2002).
[12] J. Colin et al., Phys. Rev. C **67**, 064603 (2003).
[13] S. Piantelli et al., Phys. Rev. Lett. **88**, 052701 (2002).
[14] E. D. Filippo et al., Phys. Rev. C **71**, 044602 (2005).
[15] G. Casini et al., Phys. Rev. Lett. **71**, 2567 (1993).
[16] A. B. McIntosh et al., Phys. Rev. C **81**, 034603 (2010).
[17] T. Paduszynski et al., Nucl. Instr.and Meth. A **547**, 464 (2005).
[18] P. Glässel et al., Z. Phys. A **310**, 189 (1983).
[19] J. Lecolley et al., Phys. Lett. B **354**, 202 (1995).
[20] C. P. Montoya et al., Phys. Rev. Lett. **73**, 3070 (1994).
[21] P. Russotto et al., Phys. Rev. C **81**, 064605 (2010).
[22] C. Sfienti et al., Phys. Rev. Lett. **102**, 152701 (2009).
[23] S. Hudan et al., Phys. Rev. C **71**, 054604 (2005).
[24] D. J. Hinde et al., Phys. Rev. C. **39**, 2268 (1989).
[25] P. Grangé and H. A.Weidenmüller, Phys. Lett. B **96**, 26 (1980).
[26] P. Grangé et al., Phys. Rev. C **34**, 209 (1986).